Arab J Geosci (2017) 10: 72
DOI 10.1007/s12517-016-2817-8

ORIGINAL PAPER

Mineralogy, geochemistry, and ore formation of Nuwaifa bauxite deposit, western desert of Iraq

Thair Al-Ani[1]

Received: 2 February 2015 / Accepted: 26 December 2016 / Published online: 10 February 2017

Abstract Nuwaifa Formation is a part of sequence stratigraphy that belongs to the Jurassic system exposed in the western desert of Iraq. The Jurassic system consists of Ubaid, Hussainiyat, Amij, Muhaiwir, and Najmah formations. Each formation is composed of basal clastic unit overlain by upper carbonate unit. Nuwaifa karst bauxite was developed in fossil karsts within the Ubaid Formation in areas where maximum intersection of fractures and faults exist. This bauxitization process affected the upper surface of the Ubaid limestone formation, which directly underlies the Nuwaifa bauxite Formation. Nuwaifa Formation represents karst-filling deposit that consists of a mixture of allochthonous (sandstone, claystone, and mudstone) and autochthonous lithofacies (bauxite kaolinite, kaolinitic bauxite, iron-rich bauxite, and flint clay). Most bauxite bodies occur within the autochthonous lithofacies and are lenticular in shape with maximum thickness ranges from few meters to 35 m and in some place up to 100 m. Petrographically, the bauxite deposit exhibits collomorphic-fluidal, pisolitic, oolitic, nodular, brecciated, and skeletal textures indicative of authigenic origin. Mineralogy boehmite and gibbsite are the only bauxite minerals; the former is dominant in the upper parts of the bauxite profiles, whereas the latter is dominant throughout the lower and middle part of the bauxite. Kaolinite, hematite, goethite, calcite, and anatase occur to a lesser extent. The study bauxites are mainly composed of Al_2O_3 (33–69.6 wt.%), SiO_2 (8.4–42 wt.%), Fe_2O_3 (0.5–15.9 wt.%), and TiO_2 (0.7–6.1 wt.%) with LOI ranging from 13.5 to 19.1 wt.%. Geochemical investigations indicate that the immobile elements like Al_2O_3, TiO_2, Cr, Zr, and Ni were obviously enriched, while SiO_2, Fe_2O_3, CaO, MgO, Zn, Co, Ba, Mn, Cu, and Sr were depleted during bauxitization process. The results of this study strongly suggest that the bauxite deposits of the Nuwaifa Formation are derived from the kaolinite of the Lower Hussainiyat Formation.

Keywords Karst bauxite · Allochthonous and autochthonous lithofacies · Hussainiyat region · Iraq

Introduction

The studied area is located west of Central Iraq, at about 65 km Northeast of Rutba City. Geographically, the area covers 700 km^2 with 40° 59′ to 41° 27 east longitude and from 33° 22′ to 33° 37′ north latitude (Fig. 1). The presence of the Nuwaifa bauxite Formation in the Iraqi Western Desert was reported for the first time by GEOSURV geologists (Mustafa 1991). The age of the Nuwaifa bauxites Formation was suggested as Early Eocene age on the basis of pollen analysis of the underlying and overlying rock units (Al-Rawi et al. 1997). The Nuwaifa karst bauxite was developed in fossil karsts, tens of meters deep and hundreds of meters wide, within the Ubaid Formation carbonates (Early Jurassic) in areas where maximum intersection of fractures and faults exist. Ghar Formation lies uncomfortably overlies of Nuwaifa bauxite Formation, composed mainly of sand and gravels of Pliocene age. Both contacts are unconformable, and thus, the age of Nuwaifa Formation is difficult to determine purely on the basis of stratigraphy as the time span between the underlying and overlying formations is very wide (Jurassic-Pliocene) (see Fig. 2). Most bauxite bodies are lenticular in shape with maximum thickness ranges from few meters to 35 m and in some place reach up to 100 m.

✉ Thair Al-Ani
thair.alani@gtk.fi

[1] Geological Survey of Finland, 02151 Espoo, Finland

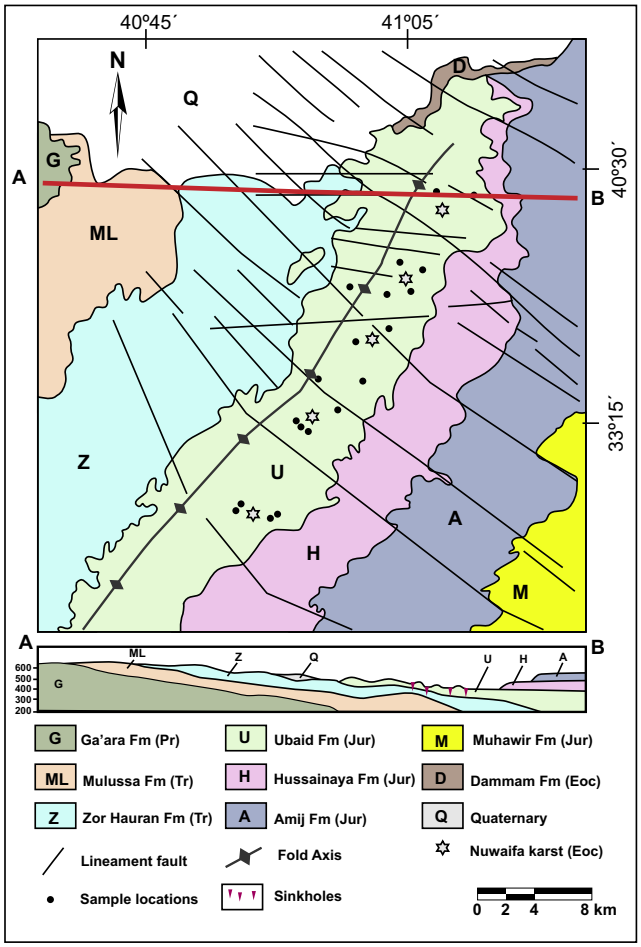

Fig. 1 Simplified geological map of the area including the limits of the geological formations, structural features, Nuwaifa karsts, and sample locations

Karst bauxite is generally produced by in situ alteration and accumulation of residual components from the leaching of either the karst-host limestone and/or the sediments filling the karst especially in case of deep sinkholes where the resulted bauxite material may remain in place after the leaching of the source rocks (Bardossy 1982; Valeton et al. 1987; Bogatyrev et al. 2009). Although most of the known bauxite deposits are lateritic type, the geochemistry mineralogy and genetic implications of many karstic bauxite deposits in the world have been well studied and examined (e.g., Liaghat et al. 2003; Mameli et al. 2007; Esmaeily et al. 2010; Liu et al. 2010a; Liu et al. 2013; Zarasvandi et al. 2008, 2010, 2012; Gu et al. 2013; Hanilci 2013; Mongelli 2002; Zamaniana et al. 2016).

In this paper, the Nuwaifa bauxite deposits of the western desert of Iraq are examined in terms of field relations, lithologic associations, petrography, mineralogy, and geochemistry. The objectives were to reveal the depositional environment and conditions of bauxite mineralization as well as to identify the immobile elements and apply their variation to trace the bauxite precursor and to follow mineralogical and geochemical evolution with increasing grade of bauxitization

Geological setting and bauxite occurrence

The studied area is part of Rutba subzone located in the Stable Shelf of the Arabian Platform (Buday and Jassim 1987). The activity of the Rutba uplift and graben during the Early Jurassic greatly affected the paleogeography and sedimentary cover of the basin in the study area.

The Nuwaifa formation is divided into two (Lower and Upper) members. The Lower Member (Lower Eocene-Upper Paleocene) is composed of bauxitic and flint clay deposits (Fig. 3a). The bauxite deposits of Nuwaifa Formation are associated with kaolinite and appear as pockets and lenses scattered throughout the karst depressions. The bauxite deposits are rather small in size, ranging from 1 to 6 m thickness. They are predominantly irregular tabular deposits surrounded by massive kaolinite (Fig. 3b). The depositional environment of bauxitic deposits is considered as karstic swamp sedimentation, while the clastic materials associated with bauxite consist of fluvial deposits. The Upper Member (Upper Eocene) is up to 85 m thick and represents the upper unit of the karst depression. The Lower part of this member composed mainly of quartoze sandstone, followed by dark red oolitic-kaolinitic sandy clay with thin horizons of ferruginous breccias. The upper part of this member consists of ferruginous multicolored sandstone, topped by red kaolinitc claystone.

Regional aspects of the lithofacies

The Nuwaifa bauxite Formation is divided into two major groups of lithofacies according to lithology. The first group is the allochthonous lithofacies (Table 1), formed mainly from clastic sediments transported during several sedimentary cycles; three lithofacies have been identified as sandstone (Chanel fill), sandy or silty claystone (flood plain), and claystone (basin of karst) lithofacies. These lithofacies are dominated by multiple sequences of fining upward sandstone with thickness between 35 and 70 m.

The second group of lithofacies in Nuwaifa bauxite Formation is the autochthonous lithofacies (Table 2). These facies are diagenetic overprints of the former grouping and reflect the varying condition of post-depositional chemical weathering. Detailed reviews of these facies were first described in detail by Al-Ani (1996) as shown in Fig. 4, and the most interesting bauxite facies were ordered as follows:

I. Kaolinitic bauxite and bauxite: characterized by pisoidal-ooidal texture; with some other colloformic textures related to bauxitization processes as well as to some diagenetic and epigenetic modifications. The facies consist mainly of boehmite and gibbsite (>10%) with some kaolinite, non-plastic, very hard with high oolitic/matrix ratios. This rock type is formed by intensive leaching within karst

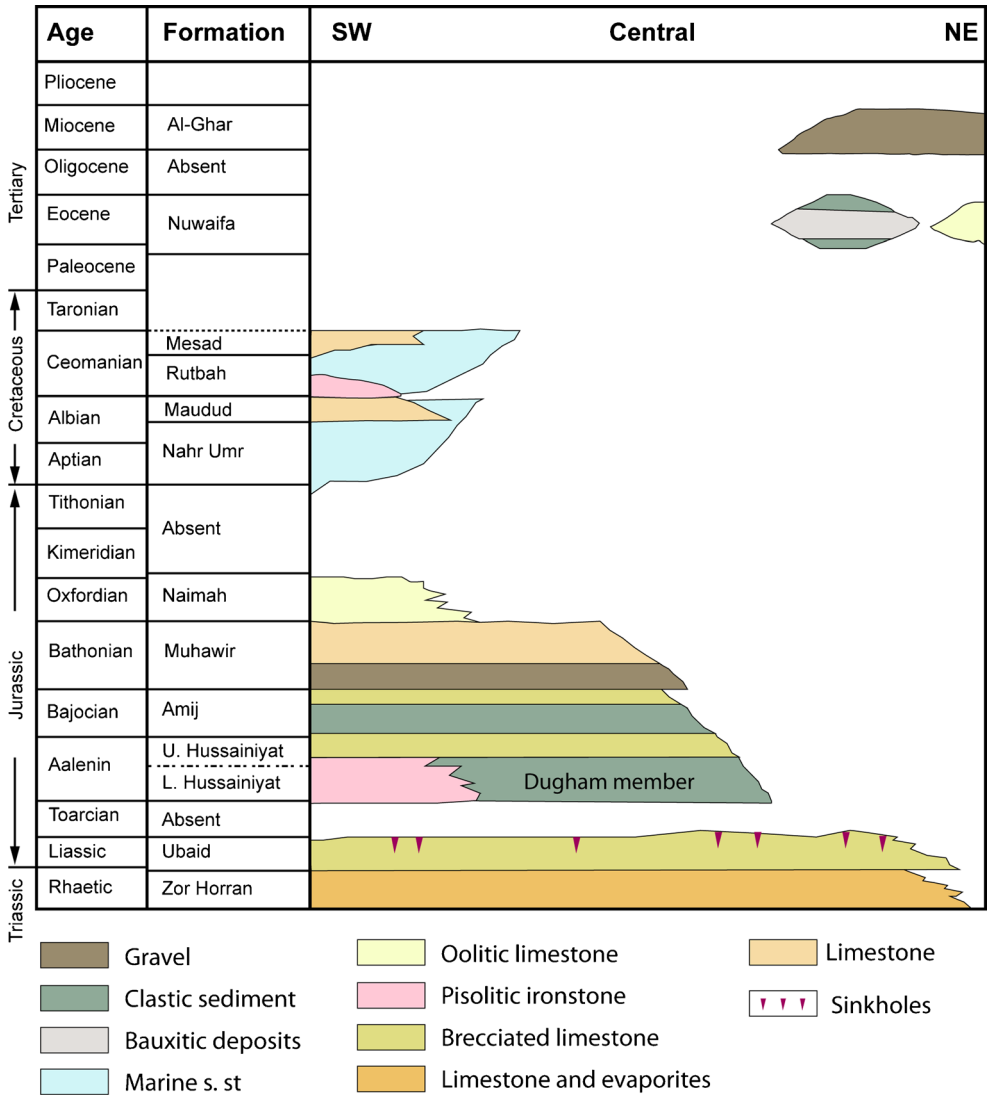

Fig. 2 Schematic diagram illustrating the stratigraphic sequence of the studied area

depression removing most of iron, silica, and other trace elements from the alluvial sediments to form low-Fe bauxite.

II. Bauxitic kaolinite: consist of kaolinite with boehmite (>10%), non-plastic, soft, white to gray in color, and with low oolitic/matrix ratios. The facies formed by chemical weathering and leaching related to strong drainage condition within the buried alluvial sediments.

III. Iron-rich bauxite: consists of boehmite, gibbsite, and disordered kaolinite with iron oxide and hydroxide minerals. Iron-rich bauxite facies is red to yellowish brown in color, soft, well segregate of iron oolites and pisolites in a matrix of high oolitic/matrix ratios.

IV. Flint clay: composed predominantly of well-crystallized kaolinite, mostly white in color, very fine grained, and hard with conchoidal fractures.

Sampling and methods

A total of about 110 rock samples were collected from trenches, sections, and boreholes from 20 different karst bauxite depressions (Fig. 1). The samples have been chosen on the basis of differences in bauxite facies (pisolitic, oolitic, brecciated, etc.) and position in the deposit. One hundred samples were selected for detailed mineralogical studies using optical microscopy. Ordinary thin sections (~30 μm thick) were observed under a petrographic microscope (LEICA IM 1000) equipped with a LEICA DFC 420 cameras for photomicrographs at the Department of Geology, University of Baghdad.

One hundred ninety (190) representative samples were characterized by XRD (powder method) using a Philips PW

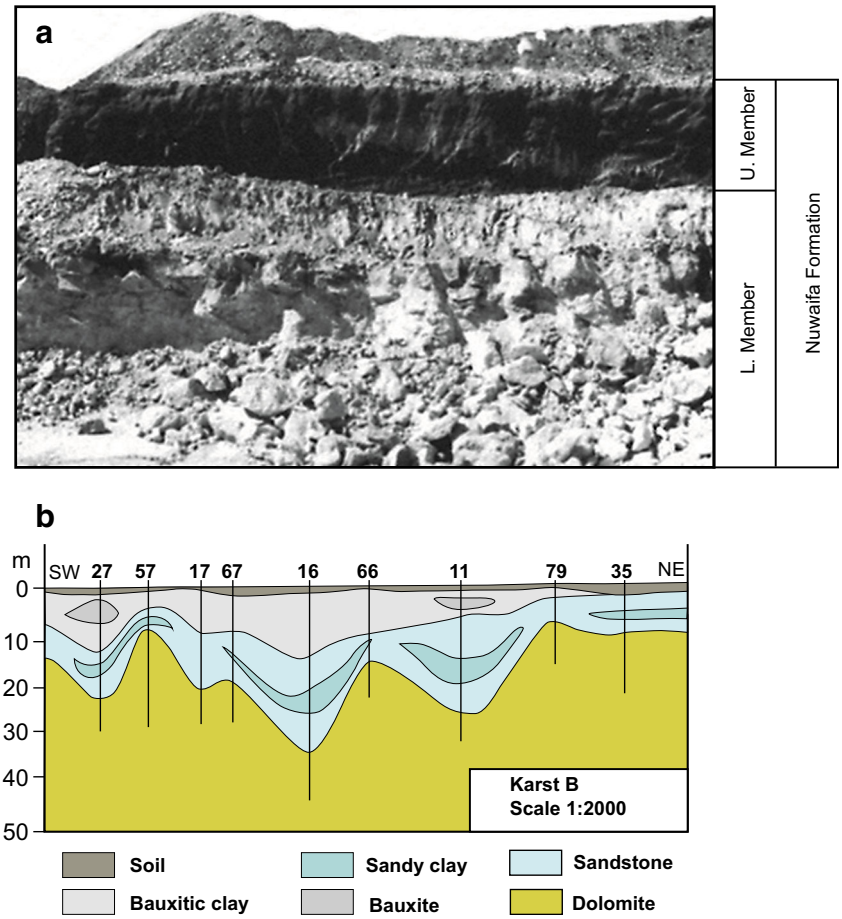

Fig. 3 **a** An exposed quarry face at Nuwaifa Formation showing bauxite and flint clay deposits of Lower Member Nuwaifa (*light color*) and clastic sediments of Upper Member Nuwaifa (*dark color*). **b** Cross-sections of karst bauxite deposits in Nuwaifa Formation

1410 X-ray diffractometer using Cu-Kα radiation at 1600 W, 40 kV, and 20 mA on powder of bulk samples and separated minerals. The clay fraction (<2 μm) was extracted by centrifuge sedimentation, and oriented aggregates (glass slide method) were prepared (Hinckley 1963) for the determination of kaolinite crystallinity index. Oriented aggregates were subjected to drying at room temperature, ethylene glycol, and heating to 550 °C and then subjected to X-ray analysis. The

Table 1 Characteristic properties of allochthonous facies within Nuwaifa Formation

Rock type	Color	Texture	Sedimentary structure	Mineralogy
Sandstone	Whitish-reddish	Mature, poorly to moderately sorted, fining upward, friable and hard at upper Part cemented by calcite or kaolinite and interbedded with laminated Fe oxides	Poorly defined planner bedding, expressed by channel forms and erosion basal contact	Quartz, calcite kaolinite with gypsum calcite as accessories
Siltstone	Reddish-brown	Moderately sorted, mature fining upward massive pisolitic hematite and veins filling by secondary calcite and gypsum	Planner bedding more common defined by thin lamination of hematitic kaolinite and siltstone	Kaolinite, quartz, hematite, with gypsum calcite as accessories
Claystone	Grayish black reddish brown at upper part	Mature, massive hard, plastic, highly fractured, contains some pisolitic hematite, brecciated textures with veins filling by calcite or quartz	Planner bedding and laminated very well defined (zonation) by alternation oh hematite, goethite and kaolinite	Kaolinite, hematite, goethite, anatase with secondary gypsum

Table 2 Characteristic properties of autochthonous facies within Nuwaifa Formation

Rock type	Color	Texture	Texture
Bauxitic kaolinite	White-gray	Oolitic-pisolitic, nodular, clayey, massive, poorly sorted with low ooids/matrix ratio, rounded and angular fragments of kaolinitic clay are scattered throughout the bauxitic-kaolin, brecciated frequently imparts a pseudo arenaceous texture, Pisolites are found randomly distributed	Well-ordered kaolinite, boehmite gibbsite and accessories of hematite, calcite and anatase
Bauxite and/or kaolinitic bauxite	White-gray with white pisolites	Oolitic-pisolitic, nodular, massive, very hard, good sorted high ooids/matrix ratio with an politic matrix, pisolites distributed randomly with size range from several mm to several cm (>2 cm), pisolitic bauxite show irregular networks of vein lets and cracks filled by neoformed kaolinite or calcite	Boehmite, gibbsite and well-ordered kaolinite, accessories as anatase, hematite and calcite
Iron-rich bauxite	Red-brownish pink with whitish pisolites	Oolitic- pisolitic, iron nodular, clayey, massive, poorly sorted with variable density of packing and usually have randomly distributed. Pisolites, showing development of pisolites due to alteration zones of boehmite, kaolinite and hematite. The outer shell of pisolites are enriched in iron oxide materials.	Boehmite, gibbsite, disorder kaolinite hematite, goethite with accessories of anatase and calcite
Flint clay	White-gray or pink with white pisolites	Homogenous, dense, non-plastic, hard, and lustrous, breaking with pronounced conchoidal fracture. Flint clay occupies the basal part of the karst, and grades down sandy claystone containing irregular forms of vug-like cavities filled by kaolinite and iron oxides to form brecciated textures.	Well-ordered kaolinite, gibbsite, anatase with accessories of hematite and calcite

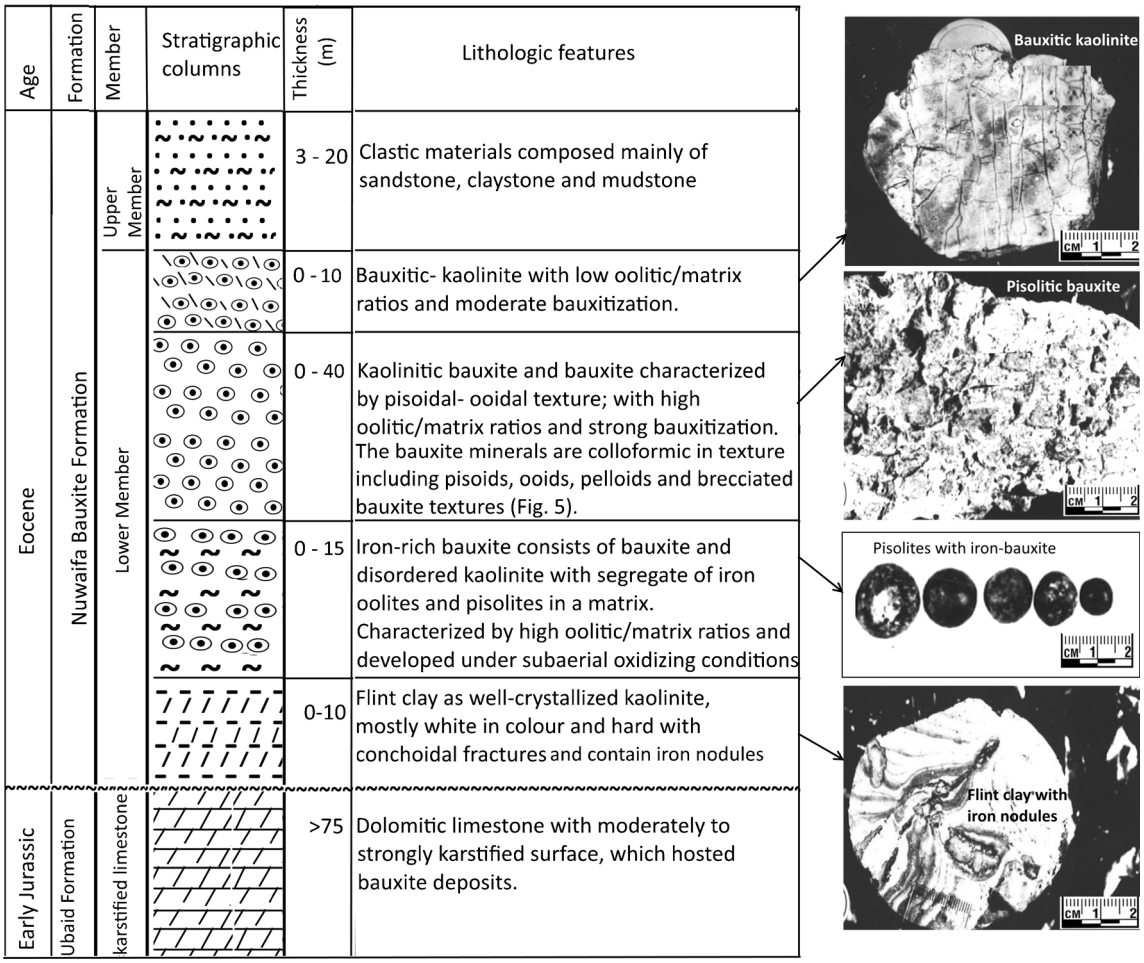

Fig. 4 Sketch map of a stratigraphic column of the Nuwaifa bauxite horizons with the main bauxitic lithofacies

iron coatings and iron mineral particles were removed from the iron-rich sample material by the technique of dithionite citrate-bicarbonate-sodium dithionite (CBD) method, in accordance with Mehra and Jackson (1960). The estimation of the iron minerals (hematite and goethite) removed can be readily determined by comparison of the X-ray diffraction patterns of the untreated sample with that of the treated samples.

Approximate mineral proportions were estimated from chemical analysis and X-ray diffractometry of bulk samples since the major and minor elements are controlled by their mineral affinities. These constituents are summarized in Table 3. The results of XRD analysis suggest that there are different mineralogical compositions or different types of investigated bauxites (Fig. 6).

Chemical analyses of major and trace elements were determined by plasma spectrometry (polyvac E 970), model Hilgar. Loss on ignition at ~1000 °C was measured gravimetrically. Analytical uncertainty, as indicated by replicated analysis, is 0.25%. The molecular ratio Ki = SiO_2/Al_2O_3 in the studied bauxite samples was used for the classification of different types of bauxites, and the ratio rw = SiO_2/Al_2O_3 + Fe_2O_3 was used to suggest the degree of weathering, which is called the weathering quotient (Schellmann 1986).

Petrography and mineralogy

The parent rocks of the studied bauxite are kaolinite-rich clastics, which are mainly composed of kaolinite (unaltered kaolinite), iron oxide minerals (goethite and hematite), and quartz with traces of illite and montmorillonite. The presence of low amount of secondary calcite filling inside the pores and fractures can be considered as related to the epigenetic process. Kaolinite, from the parent rocks, occurring as clastic particles, cementing material, and infilling of pore space or micro-veins within the bauxitic facies (Fig. 5a–d).

The petrographic studies show that the texture of the studied bauxite deposits is mainly oolitic to pisolitic, but can also change from purely oolitic to arenitic-brecciated, suggesting the reworking of evolved lateritic soils. The ooids are composed of concentric shells embedded in the matrix of recrystallized kaolinite and bauxite with traces of iron oxides (Fig. 5a). The cores of the ooids generally consist of older, detrital bauxite grains (bauxite pebbles), or of hematite-goethite fragments. The number of shells within oolites and pisolites is between 4 and 7 and the diameter range from 3 to 20 mm (Fig. 5b). Some cortices of pisolites and oolites have fractures due to synersis cracks or developed during slight compaction of the matrix. The fractures are filled by micrite and kaolinite (Fig. 5d). Composite ooids can also be noticed in the studied bauxite. They consist of several small ooids enveloped by concentric lamellae (Fig. 5c), which may be the product of syndepositional deformation and a discontinuity during the growing process of the ooids. Boehmite and hematite are more abundant in the ooids, whereas kaolinite is found at higher levels in the groundmass. However, in the structure of most ooids, boehmite and kaolinite are concentrically zoned, following a well-known diagenetic pattern (Bardossy 1982).

Colloform texture is especially common in the iron-rich bauxite facies, originated from precipitation and aging of mixed colloidal Al- and Fe-rich solution migrated in the bauxite horizons and coexists with bauxitization processes at different stages of dehydration, recrystallization, and segregation (Fig. 5e).

In addition, various colloform textures of irregular shape are common such as flow-like and stratified textures (Fig. 5f). These types of textures observed mainly in bauxite samples contain gibbsite as the dominant mineral. Intensive solution within the karst may breccias-like texture of overlying strata to collapse, which is represented by pseudomorphous textures consisting of poorly rounded and angular fragments of kaolinite, calcite, and bauxite (Fig. 5g). Brecciated textures representing the stage of mechanical disintegration immediately preceding chemical weathering are also common. The brecciated fragments embedded in the studied bauxites are optically being as isotropic crystals (Fig. 5h).

Bauxite minerals

Boehmite is the dominant bauxite mineral in the Nuwaifa Formation (Fig. 6). It was found in all of the studied bauxite samples, while gibbsite is found only in 35%. The vertical

Table 3 Mineralogical compositions of the autochthonous facies in Nuwaifa Formation

Rock type/facies	Ki = SiO_2/Al_2O_3		Mineralogy wt%					
	Range	Average	Boehmite	Kaolinite	Quartz	Calcite	Fe oxides	Anatase
Low Fe-bauxite	0.2–0.7	0.5	25.1–78.2	16.0–65.1	0.0	0.5–3.0	0.8–3.5	3.0–5.9
High Fe-bauxite	0.5–0.6	0.6	23.5–45.8	21.5–56.5	0.0	0.9–12.1	12.2–25.5	1.5–2.5
Bauxitic kaolinite	0.7–1.0	0.9	8.5–24.5	65.0–86.5	0.0	0.7–4.8	1.5–17.5	1.0–2.1
Flint clay	1.1–1.2	1.1	0.0–5.5	90.0–95.0	0.0–2.8	1.2–2.7	0.5–2.8	0.9–3.0
Weathered clay	1.0–1.5	1.2	0.0	92.1–94.1	0.0–0.4	0.5–1.3	4.5–9.6	2.2–3.2

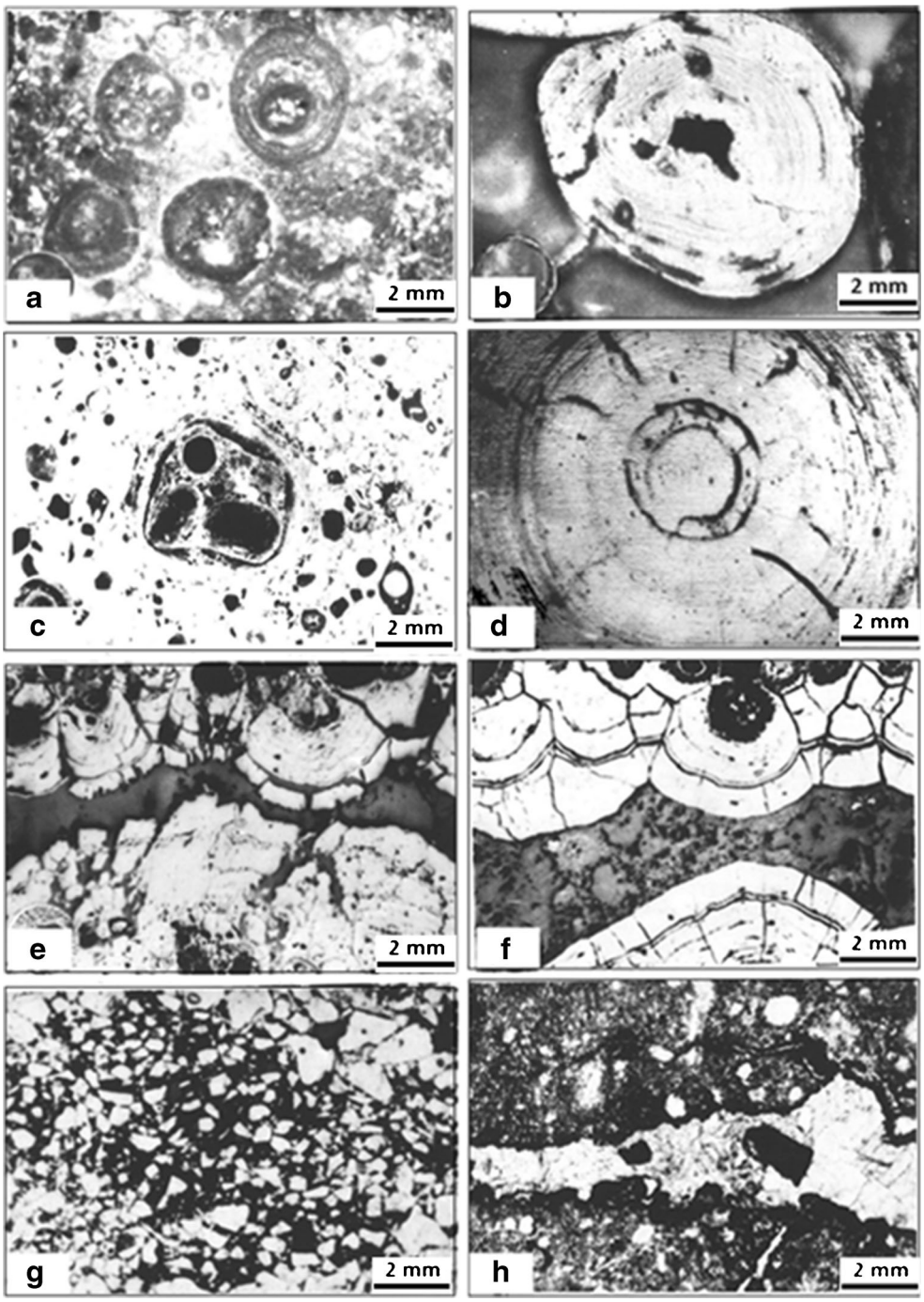

Fig. 5 Petrography of the studied bauxite using LEICA IM 1000 microscope. **a**, **b** Pisolitic bauxite embedded in a matrix made of kaolinite and iron oxides ((PPL). **c** Development of composite pisolites embedded in a matrix made of kaolinite and iron oxides (PPL). **d** Coarse pisolite shows fractures filled by micrite and kaolinite. **e**, **f** Colloform goethite with the development of syneresis cracks (XPL). **g**, **h** Brittle deformation results in brecciated bauxite texture (XPL)

distribution of boehmite and gibbsite in the studied bauxite profile of the Nuwaifa Formation does not follow a specific pattern (Fig. 7). Boehmite content increases in the upper parts of the bauxite profiles, whereas gibbsite is dominant throughout the lower and middle part of the bauxite profiles (Al-Ani 1996). According to Bardossy (1982), boehmite formed in the zone of leaching (above the water table) and gibbsite in the zone of saturation (below the water table). Kittrick (1969) conclude that amorphous aluminum hydroxide or gibbsite (primary bauxite) was formed directly from kaolinite after removing of silica. Kaolinite dissolves incongruently to give gibbsite (as residue material) and amorphous silica (as aqueous) in solution; boehmite product is probably due to the dehydration of gibbsite.

According to the following chemical equation (modified from Bardossy 1982), the desilication of parent rocks (kaolinite) is usually a two process in which hydrous aluminum oxides are formed first and then silica is removed from them to form gibbsite, and continued loss of silica from kaolinite produced boehmite, and diaspore.

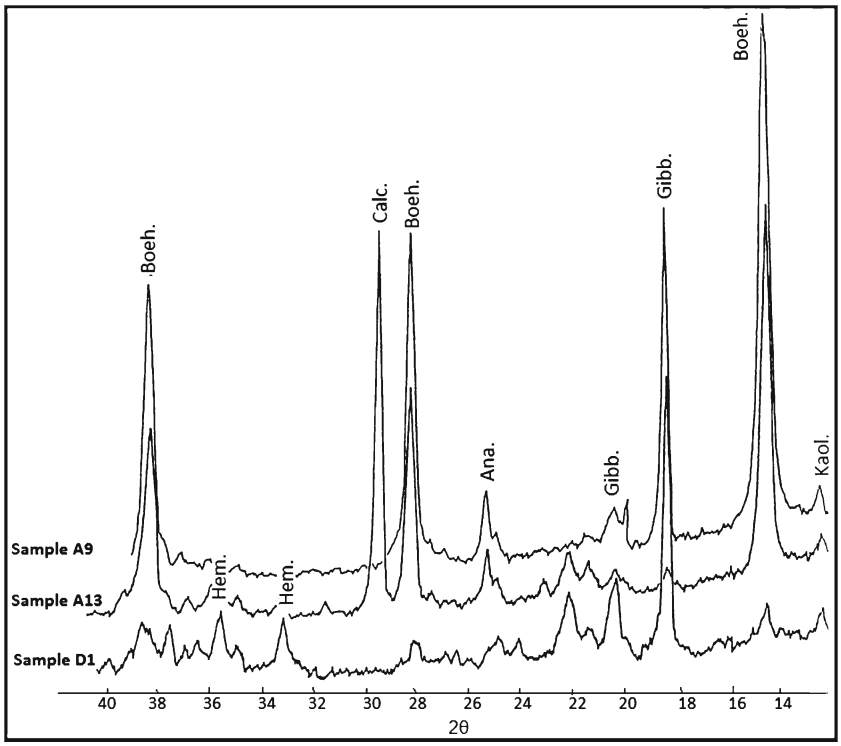

Fig. 6 XRD patterns of three bauxite samples. *Boeh.* boehmite, *Gibb.* gibbsite, *Kaol.* kaolinite, *Hem.* hematite, *Gth.* goethite, *Calc.* calcite, *Ana.* anatase

Kaolinite → gibbsite + amorphous silica → boehmite → diaspore

$Al_2Si_2O_5(OH)_4$ $Al(OH)_3 + H_4SiO_4$ (*aqueous*) $Al_2O_3{\cdot}3H_2O$ $Al_2O_3{\cdot}H_2O$

The abundance of bauxite minerals (boehmite and gibbsite) within the studied lithofacies varies over a wide range: low Fe-bauxite 25–78 wt.%, high Fe-bauxite 23.5–45.8 wt.%, bauxitic kaolinite 8.5–24.5 wt.%, and flint clay 0.8–5.5 wt.% (Table 3). Low iron bauxite of the studied karst depressions may have been formed under reducing conditions which caused Al enrichment and the removal of Fe from kaolinitic sediments to form the white colored bauxite with boehmite is the principal component (Kloprogge et al. 2002). The Fe-rich bauxite of some studied profiles indicates

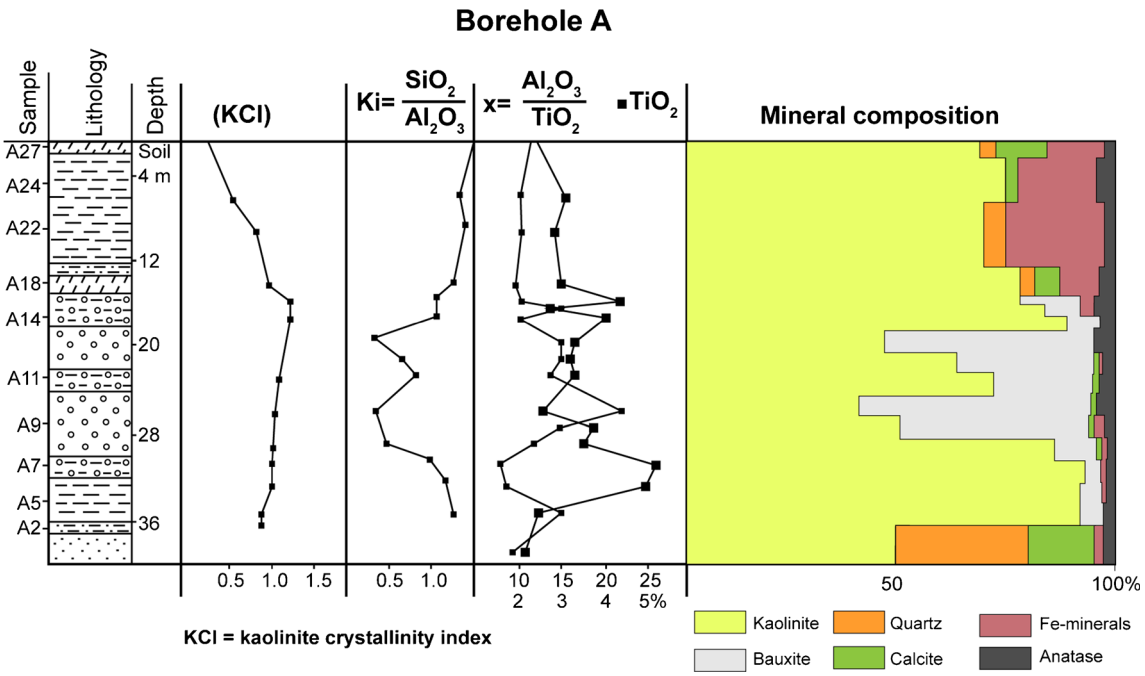

Fig. 7 Vertical profiles of crystallinity index of kaolinite (KCl), SiO_2/Al_2O_3, Al_2O_3/TiO_2 ratios, TiO_2 value, and mineral composition in the Nuwaifa Formation

under oxidizing conditions in temporary fresh water basins and derived from Fe-rich source materials of Hussainiyat ironstone Formation. Similar conclusions were arrived by Schorin and Puchelt (1987), which mentioned that the ferruginous bauxite from southeast Venezuela was deposited on land, under oxidizing conditions in temporary fresh water basins.

Kaolinite:

Kaolinite is almost the only clay mineral found in the studied rocks, with traces of mixed layer of illite-smectite. Kaolinite occurs as clastic particles in allochthonous and autochthonous lithofacies, as reworked fragments, as in situ (new formed) oolites and as late diagenetic infilling of pore spaces and microveins. The percentage of kaolinite within studied lithofacies are 16–65 wt.% in low Fe-bauxite, 21.5–56.5 wt.% in high Fe-bauxite, 65–86.5 wt.% in bauxitic kaolinite, and 90–95 wt.% in flint clay (Table 3).

Crystallinity index of kaolinite (KCI) determination was measured using the method described by Hinckley (1963). This index is the ratio of the sum of the heights of the reflections (1$\grave{1}$0) and (11$\grave{1}$) measured from the inter-peak background, and the height of the (1$\grave{1}$0) peak measured from the general background (Fig. 8).

The entire spectrum of crystallinity values from poorly crystallized kaolinite (disordered) to well crystallize kaolinite (very well ordered) was encountered within the karst bauxite profiles as follows:

(a) Kaolinite is poorly too moderately and poorly crystallized in clays of allochthonous facies. Reported values range from 0.3 (disordered) to 0.8 (ordered).
(b) Kaolinite is very well crystallized in bauxitic kaolinite, bauxite, and flint clay. Crystallinity values range from 0.6 (ordered) to 1.4 (very well ordered). These facies were generated by the most intensive chemical weathering, and well-crystallized kaolinite was formed by the removal of alkalis and silica to produce authigenic kaolinite as suggested by Bardossy (1989) elsewhere.
(c) Kaolinite is poorly crystallized in iron-rich bauxite facies. Reported values range from 0.3 to 0.6 with an average around 0.45. These facies were generated by most intensive diagenetic reorganization under oxidizing condition. The presence of iron oxides associated with clay particles affected the crystallinity of kaolinite, which are generally more disordered than in the low-iron bauxite facies.

Iron oxide minerals

Hematite and goethite are common authigenic minerals in the studied rocks. Hematite is the main Fe-mineral in the studied stratiform and karst bauxites, present in the pisoids, ooids, and matrix. In the studied bauxite profiles, hematite content decreases as bauxite minerals increase. Source rocks contain about 3.5% hematite, depleted to 1.1% in the low Fe-bauxite. This trend of continuous Fe-leaching during bauxitization suggests reducing conditions during the process. Hematite content is higher in the pisoidal-ooidal bauxites than in the massive varieties. Abundant angular fragments of hematite and goethite occur as millimeter-sized clasts in the studied bauxite and also detrital hematite-goethite fragments in the ooids.

Iron-rich bauxite facies contain hematite which has some aluminum as an isomorphic substituent. This variety is called alumohematite (Bardossy 1982). The XRD analyses of selected iron-rich samples (PH 19/8 and PH 2/1) revealed that hematite and goethite are the major Fe-mineral components in the studied bauxite deposit (Fig. 9). A shift of all peak positions to larger 2θ values is observed with increasing Al substitution due to the difference in the ionic radii of the Fe and Al cations, indicating that Al is incorporated into the structure of hematite to produce alumohematite. The XRD reflections of alumohematite represent higher θ2θ values depending on the degree of aluminum substitution (Fig. 9a).

Goethite is the second most frequent iron mineral of karst bauxite next to hematite. The bulk of goethite (both syn- and diagenetic) is the result of pyrite oxidation. Also, Fe is replaced by Al to produce alumogoethite especially in iron-rich bauxite facies (Fig. 9b). The color of Fe-rich bauxite, which is red or violet in some of the studied bauxite samples, may thus be a function of the degree of aluminum substitution (Meyer et al. 2002).

Titanium minerals

Anatase is the only titanium mineral detected in the studied samples. The Nuwaifa karst bauxites are strikingly rich in anatase (3.0–5.9). Most of anatase in the studied bauxite is syngenetic in origin, finely dispersed in the matrix, with a particle size of 0.1–1.0 μm. The abundance of anatase is somewhat more common in the matrix materials than in the concentric particles (oolites, pisolites).

Quartz

Quartz occurs as fine (<0.01 mm) clastic grains and usually subrounded to subangular, acicular rutile, or tourmaline imbedded inclusion within coarse-grained quartz. The contact between the quartz grains is mostly straight, although some contacts show either concave or convex pattern in the alllochthonous facies. Quartz was absent in most of the bauxite facies due to its stronger corrosion and partial replacement by gibbsite and boehmite.

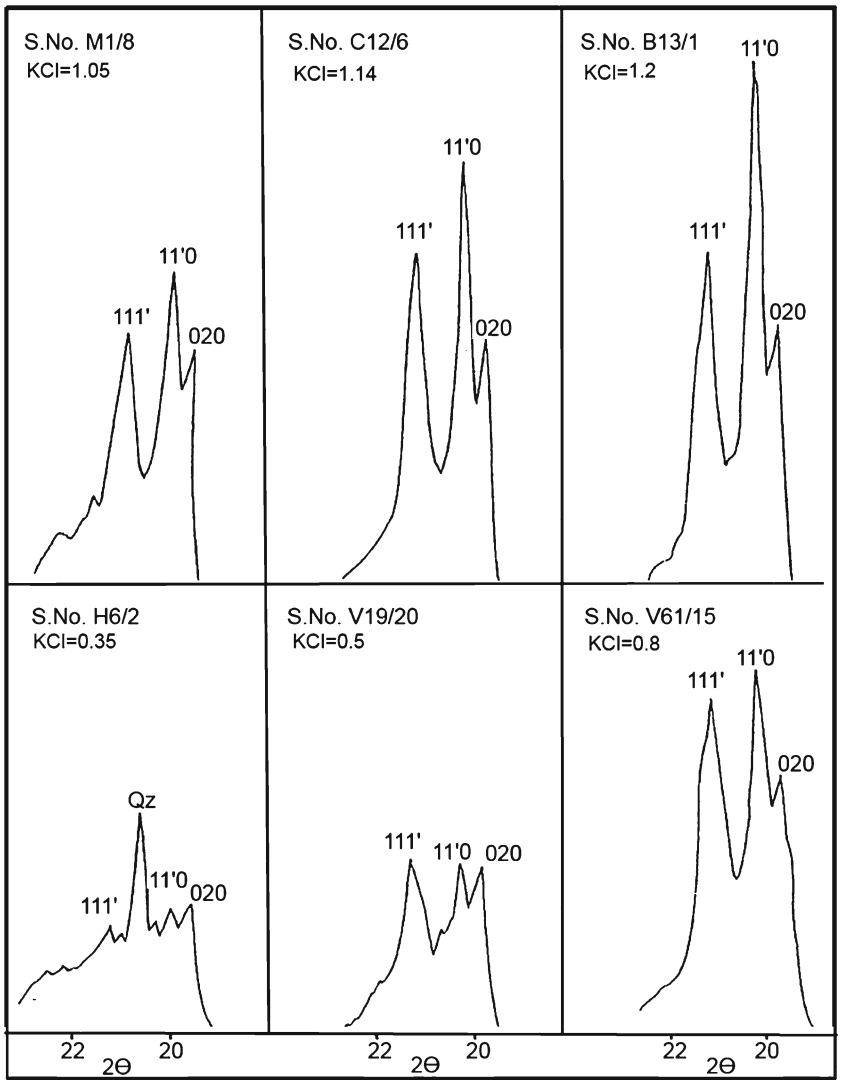

Fig. 8 XRD patterns of kaolinite in different kaolinite crystallinity index (KCI = 1Ì0 + 11Ì/1Ì0) charts according to Hinckley (1963)

Calcite

As mentioned above, the bauxitization in the study area is developed within the Ubaid Formation carbonates (Early Jurassic) in areas where maximum intersection of fractures and faults exist. Most of the calcite in Nuwaifa karst bauxite is of diagenetic and epigenetic origin, formed out of ground water seeping down from a carbonate cover, and precipitated as secondary calcite filling the fissures and cracks in the kaolinitic and bauxite facies.

Geochemistry

Ninety-two rock samples are chemically analyzed for major oxides (Al_2O_3, SiO_2, Fe_2O_3, TiO_2, CaO, MgO, SO_3, K_2O, and L.O. I) and trace elements (Zn, Co, Ni, Ba, Mn, Cr, Sr, and Zr) on studied bauxite deposits to shade some light into the environment of deposition as well as on the origin of the deposits. Four bauxitic facies were identified in Nuwaifa Formation. Each one has high aluminum (53.1 wt.% Al_2O_3) and low silica contents (22.7% of SiO_2) as in kaolinitic bauxite facies. Analytical data relative to the various autochthonous bauxite facies are listed in Table 4. In the present study, average chemical composition of unaltered kaolinite within Nuwaifa Formation was used to represent source rocks for low Fe-bauxites, and average chemical composition of samples collected from the iron-rich kaolinitic rocks of the neighboring Hussainiyat Formation was used to represent source rocks for the high Fe-bauxites.

Using ternary plots of Al_2O_3–Fe_2O_3–SiO_2 (Aleva 1994) unveils some important points concerning the chemical characteristics of the bauxite ores. The Nuwaifa bauxite data points on these plots show that the ores have bauxite to kaolinitic bauxite compositions with few samples in buaxitic kaolinite field (Fig. 10a). Plots of the Nuwaifa bauxite data on the of Al_2O_3–Fe_2O_3–SiO_2 triangular diagram (Fig. 10b) illustrated different degrees of the lateritization (Schellmann

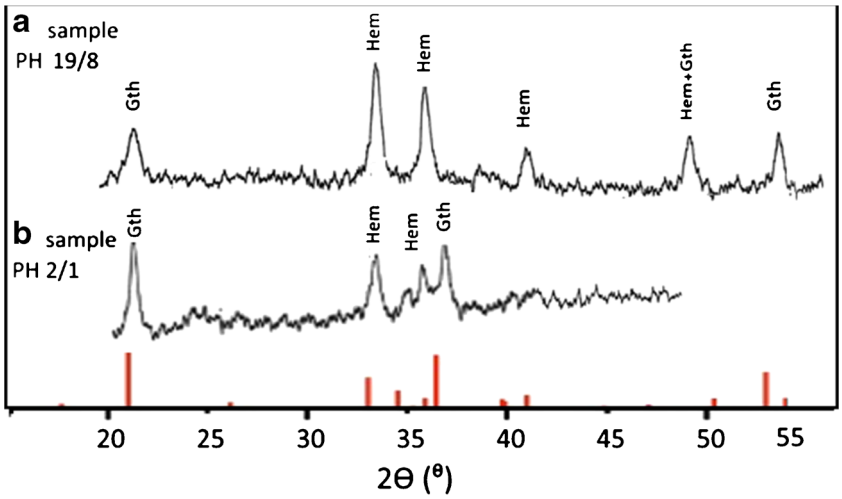

Fig. 9 X-ray powder diffraction patterns for iron-rich samples **a** PH 19/8 and **b** PH 2/1. *Red vertical lines* show the XRD pattern from the standard hematite and goethite

1982). In this diagram, Al_2O_3-rich samples experienced of higher degrees of lateritization, while SiO_2-rich samples are indicative of a weaker degree of lateritization (Meyer et al. 2002). In addition, the samples show that the Nuwaifa bauxite deposit was the product of moderate to strong lateritization. Moreover, MacLean et al. (1997) proposed that the immobile elements can even be used to trace the source of aluminum to a particular rock type or unit. In the Ni–Cr diagram (Fig. 11), pisolitic-rich bauxite samples of Nuwaifa Formation are through karst bauxite field or close to the karst bauxite field with a shale and/or slate that might be the possible parent rocks.

The concentration ratios of chemical changes during bauxitization were assessed using enrichment factors (C_b/C_k), which the ratio between the content of an element in any is given bauxitic facies Cb and that of the parent rock Ck.

The average concentration and depletion ratios with respect to the proposed kaolinite (within karst depressions) as source rock for the various autochthonous bauxite facies (C_b/C_k) are presented in Table 5. Values >1 represent enriched elements whereas values <1 represent leached out ones. The most studied bauxite samples are enriched in the immobile elements (Al, Zr, Ti, Ni, Cr, and H_2O) and depletion of mobile elements Fe, Ca, Mg, Si, Cu, Zn, Co, Sr, Ba, and Mn. The results show

Table 4 Major and minor elements in bauxite facies and in the source rock of Nuwaifa Formation

Oxides/ elements	Kaolinitic bauxite	Separated pisolites	Bauxitic kaolinite	Iron-rich bauxite	Flint clay	Source rock	
						Low Fe-bauxite	High Fe-bauxite
wt%							
SiO_2	14.0–32.0	10.2	32.0–41.0	9.8–26.4	41.3–44.0	44.4	38.6
Al_2O_3	46.1–62.2	62.3	39.1–45.0	37.0–51.5	36.0–39.5	34.4	32.7
Fe_2O_3	0.3–2.5	1.6	0.3–5.6	11.2–23.0	0.4–3.5	3.5	9.3
TiO_2	2.0–6.0	2.3	1.5–4.4	1.6–3.5	1.5–3.9	2.5	1.8
CaO	0.1–3.6	0.4	0.2–1.1	0.5–6.5	0.1–0.9	0.5	1.2
MgO	0.1–0.2	0.2	0.1–0.2	0.1–0.2	0.1–0.3	0.3	0.2
L.O. I	14.0–22.3	20.2	11.5–19.1	12.6–21.0	13.1–15.0	13.3	13.5
Ppm							
Zn	25–100	89	34–170	33–40	31–213	93	155
Co	12–68	23	25–68	19–38	25–125	51	40
Ni	20–80	27	41–108	42–63	28–180	50	61
Ba	2–95	16	2–155	39–95	15–144	82	83
Mn	3–34	15	11–45	20–28	9–60	53	59
Cr	130–335	296	142–254	225–330	140–275	190	235
Cu	6–30	7	2–46	46–110	2–44	22	78
Sr	6–99	64	36–212	26–80	19–145	125	67
Zr	80–337	66	30–183	208–272	50–220	61	98

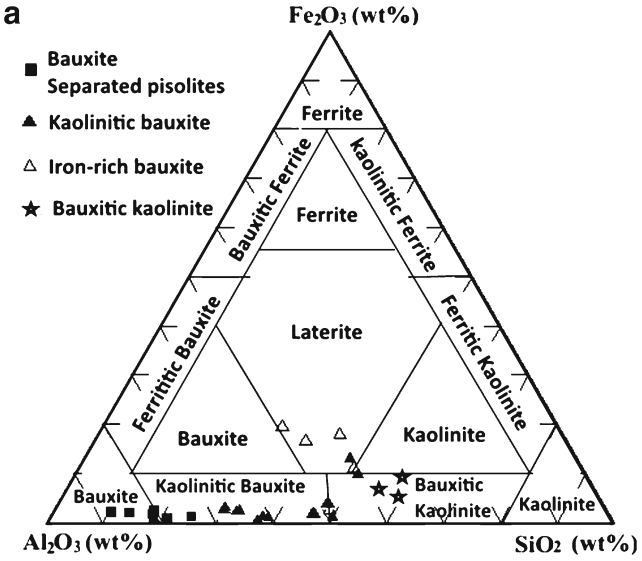

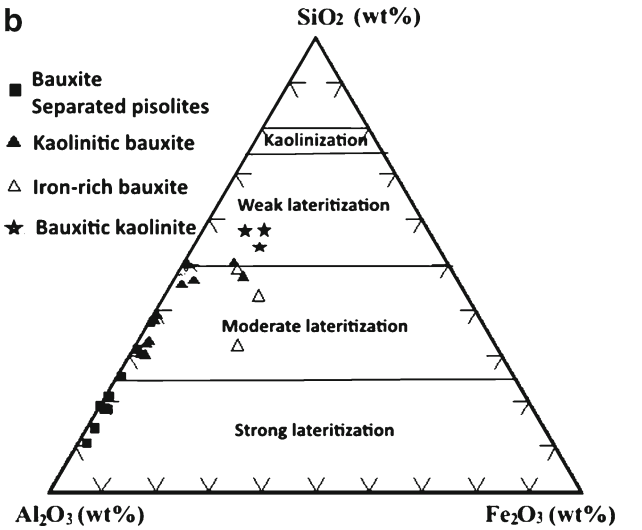

Fig. 10 The Fe_2O_3–Al_2O_3–SiO_2 triangular diagrams showing **a** the mineralogical classification of the bauxite ores (after Aleva 1994), **b** degree of lateritization (after Schellmann 1982) in the Nuwaifa bauxite Formation

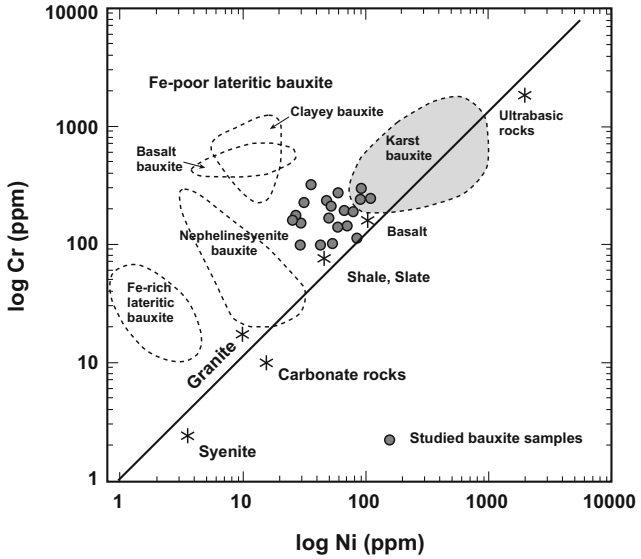

Fig. 11 Plot of Ni versus Cr concentration values for various types of bauxites in relation to various precursor rocks (after Schroll and Sauer 1968)

that Zr was enriched more than Al in all bauxite facies. The enrichment values of Zr of the kaolinitic bauxite and iron-rich bauxite (C_b/C_k = 2.93 and 2.44, respectively) are higher than those of the bauxitic kaolinite and flint clay facies (C_b/C_k = 1.88 and 1.74, respectively). Ni is more enriched than Al in bauxitic kaolinite and flint clay facies (C_b/C_k = 1.26 and 1.38, respectively), whereas in kaolinitic bauxite and iron-rich bauxite facies, Ni is less enriched than Al (C_b/C_k = 1.1 and 0.85, respectively). Although alumina is the main chemical component of bauxite, its enrichment relative to the parent rock is more restricted than that of Zr and Ni (Table 5, such as in bauxitic kaolinite and flint clay facies). Some trace elements were depleted during the bauxitization process. This represents a little leaching of the initial silica content especially in bauxitic kaolinite (C_b/C_k = 0.84) and flint clay facies (C_b/C_k = 0.93) and leaching of significant amount of silica from the kaolinitic bauxite (C_b/C_k = 0. 53) and iron-rich bauxite (C_b/C_k = 0.23).

The values for the molecular ratio Ki approaches 2.0 for pure kaolinite and zero for pure alumina (diaspore). Comparing the variation in molecular ratios of selected bauxite facies with the source materials (kaolinite of the neighboring Hussainiyat Formation and weathered clay within the Nuwaifa Formation (Table 6 and Fig. 7) show decline in their averages in the average values of Ki and rw from flint clay (1.14 and 1.06, respectively) to bauxitic kaolinite (0.91 and 0.87, respectively) to kaolinitic bauxite (0. 55 and 0.43, respectively). These changes result from the breaking up of the aluminosilicate constituents of the unaltered clays within the Nuwaifa Formation during its weathering under tropical conditions to form the bauxite ore.

Mineral genesis and ore-forming environment

The mineralogical and geochemical data obtained in this study suggest that Nuwaifa bauxite Formation in the Western Desert of Iraq is similar to other mineable bauxite deposits in the world, such as in Zagros Mountain Belt, southern Iran as the bauxitic–lateritic deposits (Zarasvandi et al. 2008), Mombi bauxite deposit, Zagros Mountains, Iran as typical of the karst type (Zamaniana et al. 2016), Caribbean bauxite ore province, Jamaica Island (Bardossy 1982), southern Spain (Molina et al. 1991), Weipa bauxite, northern Australia (Taylor et al. 2008a, b), Sardinia (MacLean 1990; MacLean et al. 1997), and southern Italy (Mongelli 2002). The mainly oolitic–pisolitic textures of the studied bauxite, their lack of graded- or cross-bedding, plus the presence of boehmite, a common Al-rich

Table 5 Average concentration ratios (C_b/C_k) of major and minor elements in autochthonous facies as compared with kaolinite source rocks enriched elements ($C_b/C_k > 1$), depleted elements ($C_b/C_k < 1$)

	Elements	Kaolinitic bauxite	Iron-rich bauxite	Bauxitic kaolinite	Flint clay
Enriched	Zr	2.93	2.44	1.88	1.74
	Al	1.54	1.32	1.21	1.10
	Ni	1.10	0.85	1.26	1.38
	Ti	1.31	1.3	1.05	1.04
	Cr	1.07	1.32	1.03	1.02
	H_2O	1.30	1.05	1.13	1.05
	Fe	1.30	1.80	0.40	0.43
Depleted	Ca	0.81	0.80	0.66	0.63
	Mg	0.60	0.64	0.60	0.60
	Si	0.53	0.23	0.84	0.93
	Cu	0.63	0.92	0.77	0.86
	Zn	0.56	0.25	0.73	0.86
	Co	0.54	0.70	0.74	0.94
	Sr	0.40	0.65	0.27	0.71
	Ba	0.28	0.78	0.40	0.87
	Mn	0.22	0.40	0.26	0.50

mineral in karst depression, indicate an authigenic origin for the Nuwaifa bauxite deposits.

On the basis of mineralogy, texture, chemical composition, and physical properties, the bauxite deposits of Nuwaifa Formation contain many of the attributes, which also indicate that weathered clastic rocks of the lower Hussainiyat Formation are the original source rock from which the bauxites were derived. A few extraclasts of kaolinite and oolitic kaolinite were found scattered within the flit clay and bauxitic kaolinite deposits of the karst profiles. These extraclasts are believed to have been derived from the lower Hussainiyat Formation because of the short transport and consequent rapid deposition. Another evidence of Hussainiyat source is that the unaltered clays within Nuwaifa Formation and clays of the lower Hussainiyat show similar average values of the molecular ratios of (SiO_2/Al_2O_3 and $SiO_2/Al_2O_3 + Fe_2O_3$). This suggests that the clays of the lower Hussainiyat Formation and the Nuwaifa Formation are genetically related.

According to the ternary plots of Al_2O_3–Fe_2O_3–SiO_2, Schellmann (1982) and Aleva (1994) unveil some important points concerning the chemical characteristics of the bauxite ores. The Nuwaifa bauxite data points on these plots show that the ores have bauxite to kaolinitic bauxite compositions and formed during moderate to strong lateritization processes. During this stage, large amounts of alkalies and silica were leached out from the system, while less mobile or immobile elements such as Al^3+, Ti^4+, Cr^3+, Ni^2+, and Zr^4+ were retained in the different layers of the lateritic profiles. The main aluminum minerals of the bauxite ores formed at this stage are mainly boehmite and less gibbsite. Two phases of bauxitization can be deduced in the study area, namely reduction phase processing of low-iron bauxite and oxidizing phase processing of high-iron bauxite.

Table 6 Summary of chemical ratios within bauxitic facies and source rocks

Facies	$Ki = SiO_2/Al_2O_3$		$rw = Al_2O_3/Al_2O_3 + Fe_2O_3$	
	Range	Average	Range	Average
Source rocks				
Kaolinite of the neighboring Hussainiyat Fn.	1.16–1.96	1.44	1.04–1.45	1.22
Weathered clay within Nuwaifa Fn.	1.00–1.51	1.23	0.6–1.25	1.03
Bauxitic facies				
Flint clay	1.11–1.21	1.14	1.05–1.16	1.06
Fe-rich bauxite	1.06–1.32	1.24	0.7–1.02	0.86
Bauxitic kaolinite	0.72–1.01	0.91	0.71–1.0	0.87
Fe-rich kaolintic bauxite	0.56–0.61	0.55	0.37–0.38	0.43
Kaolinitic bauxite	0.22–0.69	0.45	0.21–0.68	0.44

Conclusions

1. Nuwaifa bauxite Formation of Early Eocene age is developed in the deep sinkholes and depressions (up to 70 m deep) in the carbonate rock zones of the Ubaid Formation (Early Jurassic) in the Western Desert. The karst-fill deposits consist of several fining upward cycles of quartzose sandstone and kaolinitic claystone (allochthonous lithofacies) with (or without) bauxite and bauxitic flint-clay lenses in the middle of the karst sinkholes.
2. Petrographic and mineralogical investigation reveals that kaolinite is the dominant clay mineral in the studied area and the boehmite is the dominant bauxite mineral with minor amount of gibbsite in the studied karst bauxites. These minerals show diagenetic textures formed by chemical and mechanical rearrangement of materials. These include the following: angular intraclasts (bauxite fragments); oolitic-pisolitic, colloform, flow-like, and brecciated textures.
3. Ferruginous bauxites in the Nuwaifa stratiform deposits were developed under subaerial oxidizing conditions and were derived from relatively Fe-rich source rocks as Hussainiyat ironstone deposits.
4. The principal chemical constituents of the bauxite are the Al_2O_3, Fe_2O_3, and SiO_2 mineralogically representing kaolinite and hydrated gibbsite and boehmite in this study. These oxides account for 80% of the bauxite of the Nuwaifa Formation. Enrichment and depletion of major and trace elements during the bauxitization process may be attributed to changes in pH and/or Eh values as well as the mobility of these elements. The following ions were enriched in bauxite Al^3+, Ti^4+, Cr^3+, Ni^2+, and Zr^4+. By comparison, the ions Si^4+, Fe^3+, Zn^2+, Co^2+, Ba^2+, Mn^2+, Cu^2+, and Sr^2+ were leached out.

Acknowledgements The author wishes to express his gratitude to Prof. Yehya Al-Rawi for his support and guidance. The laboratory work was done while the author was a member of the staff of the Baghdad University and is highly acknowledged. The author appreciates funding support from the Geological Survey of Iraq. Thanks to Dr. Mohammad Sayab at GTK for his help in formatting and general support during writing.

References

Al-Ani T (1996) Mineralogy and geochemistry of hussainiyat clays and associated bauxite and ironstone deposits-western desert of Iraq. Unpublished PhD Thesis, University of Baghdad, 180p.

Aleva GJ (1994) Laterites: concepts, geology, morphology and chemistry. International Soil Reference and Information Centre, Wageningen, p 169

Al-Rawi YT, Al-Ameri TK, Al-Ani T (1997) Age and Paleoclimatic evaluation of paleokarst deposits of the Nuwaifa formation, western desert of Iraq. Iraqi Geol Jour 28(2):84–92

Bardossy GY (1982) Karst bauxite. Bauxite deposits on carbonate rocks. In: Developments in economic geology, vol 14. Elsevier, Amsterdam, p 441

Bardossy GY (1989) Paleokarst: a systematic and regional review. Elsevier and Academia, Amsterdam-Praha, p 418p

Bogatyrev BA, Zhukov VV, Tsekhovsky YG (2009) Formation conditions and regularities of the distribution of large and superlarge bauxite deposits. Lithol Miner Resour 44:135–151

Buday T and Jassim SZ (1987) The Regional Geology of Iraq: Tectonism, Magnetism, and Metamorphism, S.E Geol. Surv. Min. Invest. (Geosurv), Baghdad, Iraq, 352P.

Esmaeily D, Rahimpour-Bonab H, Esna-Ashari A, Kananian A (2010) Petrography and geochemistry of the Jajarm karst bauxite ore deposit: NE Iran: implications for source rock material and ore genesis. Turk J Earth Sci 19:267–284

Gu J, Huang Z, Fan H, Jin Z, Yan Z, Zhang J (2013) Mineralogy, geochemistry and genesis of lateritic bauxite deposits in the Wuchuan-Zheng'an-Daozhenarea, northern Guizhou Province, China. J Geochem Explor 130:44–59

Hanilci N (2013) Geological and geochemical evolution of the Bolkardaˇgi bauxite deposits, Karaman, Turkey: transformation from shale to bauxite. J Geochem Explor 133:118–137

Hinckley DN (1963) Variability in "crystallinity" values among the kaolin deposits of the coastal plain of Georgia and South Carolina. Clay Clay Miner 11:229–235

Kittrick JA (1969) Soil minerals in the Al_2O_3-SiO_2-H_2O system and a theory of their formation. Clay Clay Miner 17:157–167

Kloprogge JT, Ruan HD, Frost R (2002) Thermal decomposition of bauxite minerals: infrared emission spectroscopy of gibbsite, boehmite and diaspora. J Mater Sci 37:1121–1129

Liaghat S, Hosseini M, Zarasvandi A (2003) Determination of the origin and mass change geochemistry during bauxitization process at the Hangam deposit. SW Iran, Geochemical Journal 37:627–637

Liu XF, Wang QF, Deng J, Zhang QZ, Sun S, Meng J (2010) Mineralogical and geochemical investigations of the Dajia Salento-type bauxite deposits,Western Guangxi. China J Geochem Explor 105:137–152

Liu XF, Wang QF, Feng YW, Li Z, Cai SH (2013) Genesis of the Guangou karstic bauxite deposit in western Henan. China Ore Geol Rev 55:162–175

MacLean WH (1990) Mass change calculations in altered rock series. Mineral Deposita 25:44–49

MacLean WH, Bonavia FF, Sanna G (1997) Argillite debris converted to bauxite during karst weathering: evidence from immobile element geochemistry at the Olmedo deposit, Sardinia. Mineral Deposita 32: 607–616

Mameli P, Mongelli G, Oggiano G, Dinelli E (2007) Geological, geochemical and mineralogical features of some bauxite deposits from Nurra (western Sardinia, Italy): insights on conditions of formation and parental affinity. Int J Earth Sci 96:887–902

Mehra OP, Jackson ML (1960) Iron oxide removal from soil and clays by a dithionite-citrate system buffered with sodium bicarbonate, 7th National Conference. Clay Clay Miner 8:317–326

Meyer FM, Happel U, Hausberg J, Wiechowski A (2002) The geometry and anatomy of the los Pijiguaos bauxite deposit, Venezuela. Ore Geol Rev 20:27–54

Molina JM, Ruiz-Ortiz PA, Vera JA (1991) Jurassic karst bauxites in the Subbetic, Betic cordillera, southern Spain. Acta Geol Hung 34:163–178

Mongelli G (2002) Growth of hematite and boehmite in concretions from ancient karst bauxite: clue for past climate. Catena 50:43–51

Mustafa MM (1991) Results of exploratory works for bauxite deposits in North Hussainiyat area. GEOSURV, int. rep. no. 1957, (in Arabic).

Schellmann W (1982) Eine neue Lateritdefinition. Geologisches Jahrbuch — Reihe D 58:31–47

Schellmann W (1986) A new definition of laterite. In: Banerji, P.K. (Ed.), Lateritization Processes, Geological Survey of India, Memoir, 120: 11–17.

Schorin H, Puchelt H (1987) Geochemistry of a ferruginous bauxite profile from Southeast Venezuela. Chem Geol 64:127–142

Schroll E, Sauer D (1968) Beitrag zur Geochemie von Titan, Chrom, Nickel, Cobalt, Vanadium und Molyb din in bauxitischen Gesteinen und das Problem derstofflichen Herkunft des Aluminiums. Travaux du ICSOBA 5:83–96

Taylor G, Eggletonb R, Fosterb L, Morganc C (2008a) Landscapes and regolith of Weipa, northern Australia. Aust J Earth Sci 55:13–16

Taylor G, Eggletonb R, Fosterb L, Tilleyb D, Le Gleuherb M, Morganc C (2008b) Nature of the Weipa bauxite deposit, northern Australia. Aust J Earth Sci 55:45–70

Valeton I, Biermann M, Reche R, Rosenberg F (1987) Genesis of nickel lateritesand bauxites in Greece during the Jurassic and Cretaceous, and their relation toultrabasic parent rocks. Ore Geol Rev 2:359–404

Zamaniana H, Ahmadinejad F, Zarasvandi A (2016) Mineralogical and geochemical investigations of the Mombi bauxitedeposit. Zagros Mountains, Iran, Chemie der Erde 76:13–37

Zarasvandi A, Charchi A, Carranza M, Alizadeh B (2008) Karst bauxite deposits in the Zagros Mountain belt. Iran, Ore Geology Reviews 34:521–532

Zarasvandi A, Zamanian H, Hejazi E (2010) Immobile elements and mass changes geochemistry at Sar-Faryab bauxite deposit, Zagros Mountains, Iran. JGeochem Explor 107:77–85

Zarasvandi A, Carranza EJM, Ellahi SS (2012) Geological, geochemical, and mineralogical characteristics of the Mandan and Deh-now bauxite deposits, Zagros Fold Belt. Iran Ore Geol Rev 48:125–138